Rev.Adv.Mater.Sci. 18(2008) 241-247

INVESTIGATION OF THE STRUCTURE KINETICS OF CRYSTALLIZATION $Cu_{45+x}Ti_{55-x}$ ALLOYS PREPARED BY MECHANICAL ALLOYING TECHNIQUE

M.S. Al-Assiri, A. Alolah, A. Al-Hajry and M. Bououdina

Department of Physics, College of Science, King Khalid University, PO Box 9003, Abha, Saudi Arabia

Received : March 29, 2008

Abstract. Mechanical alloying (MA) technique has been used to produce amorphous phases of $Cu_{45+x}Ti_{55-x}$ (x=0, 5, 10) system. X-ray diffraction (XRD), scanning electron microscopy (SEM), transmission electron microscopy (TEM) and differential scanning calorimetry (DSC) were used to investigate the structure, microstructure and morphology as well as the thermal stability and crystallization process in such a system. No diffraction peaks corresponding to compounds from Cu-Ti system were observed throughout the amorphization reaction. The amorphous phase of $Cu_{45+x}Ti_{55-x}$ has occurred after 6 hours of milling. This MA time is unusually short for producing amorphous phases in an alloy consisting of early-late transition metals. The crystallization temperatures of the amorphous $Cu_{45+x}Ti_{55-x}$ alloys were obtained at different heating rate. The activation energies of the studied compositions were deduced using Kissinger method.

1. INTRODUCTION

Extensive studies have been performed to develop amorphous materials due to their excellent mechanical properties and hence potential candidates for many technological applications including power electronics, thin films, solar cells, sensors, glass, ceramics, plastics, etc. Alloys consisting of early-late-transition metals in particular have very interesting characteristics in this regard. Amorphous materials can be achieved by several techniques; such as Solid state reaction (SSR), Mechanical alloying (MA), Mechanical milling (MM), Fast quenching (FQ), etc. These techniques have been tried [1-7] and important results have been obtained explaining many parameters involved in the transformation from crystalline to amorphous structure in the early-late-transition metals alloys. MA technique has some advantages compared to other conventional techniques; it can produce amorphous alloys at temperatures much lower than the crystallization temperature of its constituents and the structural changes of the sample during the amorphisation reaction can be observed.

Several works on the mechanical properties and microstructures of copper-titanium binary alloys have been curried out and some interested results have been obtained [8-11]. On the other hand, it is known that, copper is one the best element to favor formation when mixed with another metal or rare earth metals and the addition of titanium is also known to strengthen copper alloys [9].

In available papers, most of the Cu-Ti alloys were prepared by fast quenching (FQ) [10-12]. In this work, three samples with composition $Cu_{45}Ti_{55}$, $Cu_{50}Ti_{50}$ and $Cu_{55}Ti_{45}$ have been studied using MA technique to produce Cu-Ti amorphous phase. The emphasis here will put on investigations of the structure of these alloys prepared by MA technique, through comparison with other investigations of the same system prepared by other techniques [11,12].

Corresponding author: M.S. Al-Assiri, e-mail: msassiri@kku.edu.sa

2. SAMPLE PREPARATION AND EXPERIMENTAL METHOD

Three samples with different compositions: $Cu_{45}Ti_{55,}$ $Cu_{50}Ti_{50}$ and $Cu_{55}Ti_{45}$ were prepared using elemental powder of copper (99.5 wt.% purity) and titanium (99.5 wt.% purity). Four g of each sample has been weighted using a high precision balance (4 digits). Then the mixture was put in a cylindrical stainless steel vial. Two stainless steel balls of diameter 1.3 cm and 8.3 g, have been used giving a ratio of balls/powder of 4.15:1. Before closing the vial, a vacuum was applied followed with a flushing with pure Argon (Ar). The above procedure was repeated 5 times to ensure the removal of air. Then the vial was closed under 1.1 atm of Ar. A Spex 8000 miller has been used. Each of these samples has been milled continuously for 2, 4 and 6 hours. XRD patterns were obtained using Shimadzu XRD-6000 with Cu K_{α} radiation. The amorphous structures of the samples was examined by TEM instrument (JEOL, TEM 1010).

The morphology throughout the amorphisation reaction of these samples was investigated by Scanning Electron Microscopy (SEM) using JSM-6360LA instrument. The thermal stability of the amorphous phase was studied using differential scanning calorymetry (DSC) using Shimadzu DSC-50 instrument at different heating rates.

3. RESULTS AND DISCUSSION

3.1. XRD analysis

Fig. 1 shows the XRD patterns of the Cu45Ti55 samples after different milling time of 0, 2, 4, and 6h. The existence of both Cu and Ti can be clearly noticed. However the intensity of the diffraction peaks of Cu is much higher than that of Ti. By increasing the milling time of the mixture for 2 hours, a drastic decrease of the intensity of Cu diffraction peaks (about 97% compared to the original Cu peak) can be observed, whereas only a little change of the Ti diffraction peaks. Moreover, the diffraction peaks becomes broad due to the crystals size reduction and accumulation of microstrain during mechanical alloying. With further milling up to 4 hours, the diffraction peaks becomes more broaden. On the other hand, the intensities of both Cu and Ti diffraction peaks are similar and the 2 main peaks of Cu and Ti join each other. Finally, after 6 hours of milling, the diffraction pattern of the Cu45Ti55 mixture shows a very broad peak around 42°. Therefore, it can be said that the amorphous phase of the Cu45Ti55 sample can be obtained after 6h of milling. The same procedure was used for the other $Cu_{50}Ti_{50}$ and $Cu_{55}Ti_{45}$ samples and again the amorphous phase occurred after 6 h of milling. The only difference is the maximum of the amorphous halo moves toward larger diffraction angles as the Cu content increases (see Fig. 2). This is related to the fact that, the 2Θ position of the maximum of the halo of the amorphous phases is strictly connected to the size of Cu which is much smaller than that of Ti. Our results are consistent with the results previously reported for the same Cu-Ti alloys prepared by different technique [13]. Throughout the amorphization reaction of these $Cu_{45+x}Ti_{55-x}$ samples, no other diffraction peaks were observed. This is a very short prepa-

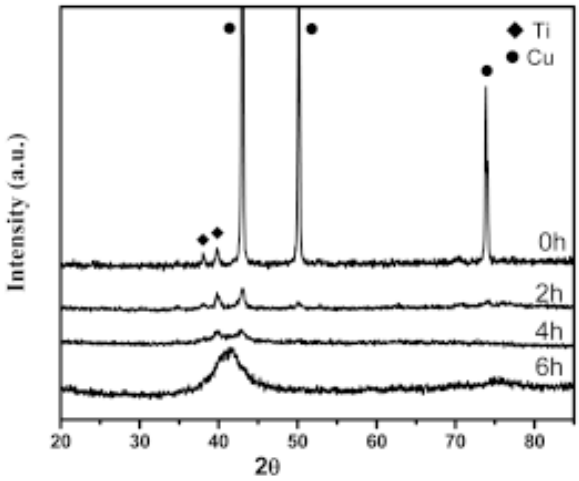

Fig. 1. XRD pattern of $Cu_{45}Ti_{55}$ sample at different miling times.

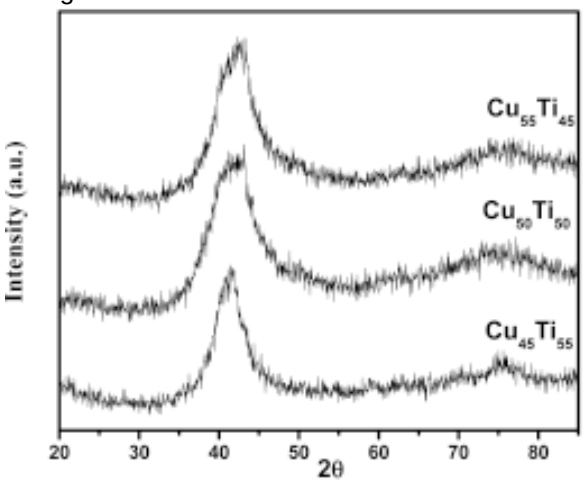

Fig. 2. XRD pattern of amorphous $Cu_{45}Ti_{55}$, $Cu_{50}Ti_{50}$, and $Cu_{55}Ti_{45}$ after 6 hours of milling.

Table 1. Chemical composition of the $Cu_{45}Ti_{55}$ mixtures determined by EDS.

Sample	No. of particle	Cu (at.%)	Ti (at.%)
$Cu_{45}Ti_{55}$ mixture as received powders	1	0.0	100.00
	2	100.00	0.0
$Cu_{45}Ti_{55}$ mixture milled for 2 hours	1	37.6	62.4
	2	46.3	53.7
	3	47.5	52.5
$Cu_{45}Ti_{55}$ mixture milled for 4 hours	1	44.2	55.8
	2	46.4	53.6
	3	42.9	57.1
$Cu_{45}Ti_{55}$ mixture milled for 6 hours	1	41.6	58.4
	2	51.4	48.6
	3	38.9	61.1

Table 2. Peak crystallization temperature T_{p1} (K) of the amorphous $Cu_{45}Ti_{55,}$ $Cu_{50}Ti_{50}$ and $Cu_{55}Ti_{45}$ powders obtained at different heating rates.

Heating rate (K/min)	Peak crystallization temperature T_{p1} (K) at different heating rate 10	15	20	25	30
$Cu_{45}Ti_{55}$	592.84	598.69	603.04	604.36	609.11
$Cu_{50}Ti_{50}$	606.71	612.88	618.46	623.28	627.78
$Cu_{55}Ti_{45}$	631.84	637.23	642.69	646.98	650.65

Table 3. E_a values of the the amorphous $Cu_{45}Ti_{55}$, $Cu_{50}Ti_{50}$ and $Cu_{55}Ti_{45}$ powders.

Sample	E_a KJ/mole	eV
$Cu_{45}Ti_{55}$	199.75	2.07
$Cu_{50}Ti_{50}$	154.25	1.60
$Cu_{55}Ti_{45}$	185.90	1.93

ration time compared with a previous study on other systems prepared by MA technique, in which the amorphous phase was obtained after very long periods of MA time [13-15]. Hence, the amorphisation treatment should be followed carefully at the early stages of the MA reaction because the short amorphisation time can be easily overshot, leading to prolonged milling periods before another amorphous phase occurred. On the other hand, this time is consistent with our recent investigations for some binary systems prepared by MA technique [16-18].

3.2. Microstructure

All the $Cu_{45+x}Ti_{55-x}$ (x=0, 5, 10) samples were examined using SEM after different milling time. The chemical analysis was deduced for such samples using EDS. Here we will present an example (which is $Cu_{45}Ti_{55}$ sample) of these SEM images accompanied with the EDS analysis where there is no much difference between the SEM results for the three samples. Fig. 3 shows the SEM images of the as received Cu_{45} Ti_{55} samples (i.e. 0 h). It can be noted that (Fig. 3a) the Ti particles are much larger than Cu ones and there is an inhomogeneous particle size distribution, whereas Cu particles show much homogeneous size distribution, the average particle size is higher than 100 μm. At higher magnification, images indicate that the Ti particles make a group of an overlapped flakes (Fig. 3b) whereas, Cu particles reveal a dendrite shape (Fig. 3c). After 2 hours of milling, there is a reduction in particle size with a more homogenous particle size distribution as shown in Fig. 4. It looks like that Cu and Ti particles reacted during milling to form a single type of particles. Images at higher magnification reveal the disappearance of the Cu dendrite-

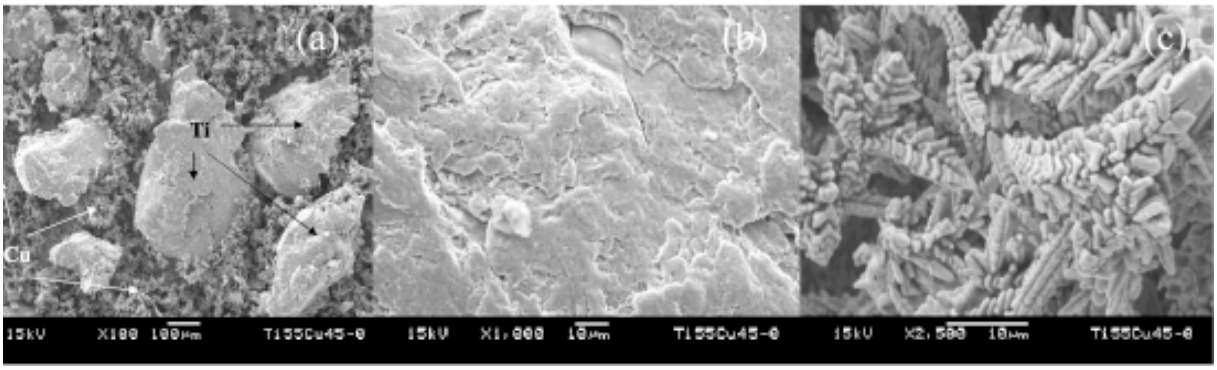

Fig. 3. SEM images of the as received $Cu_{45}Ti_{55}$ sample at different magnifications.

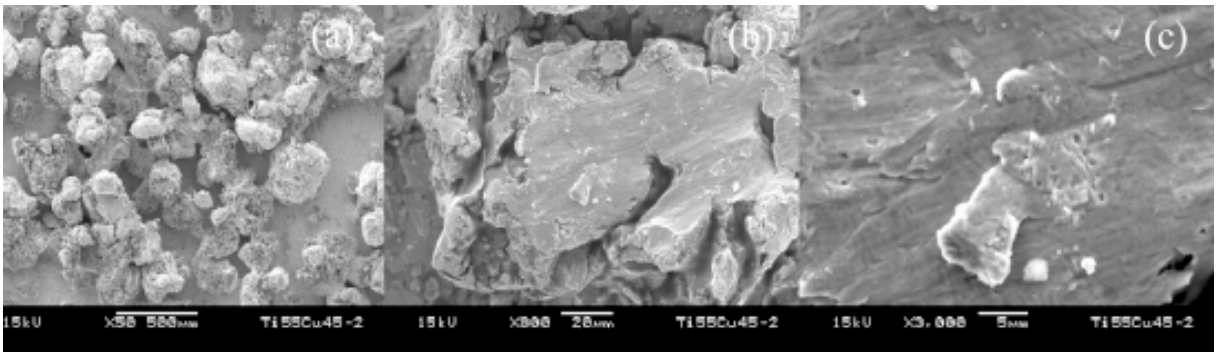

Fig. 4. SEM images of the $Cu_{45}Ti_{55}$ sample after 2 h of MA time at different magnifications.

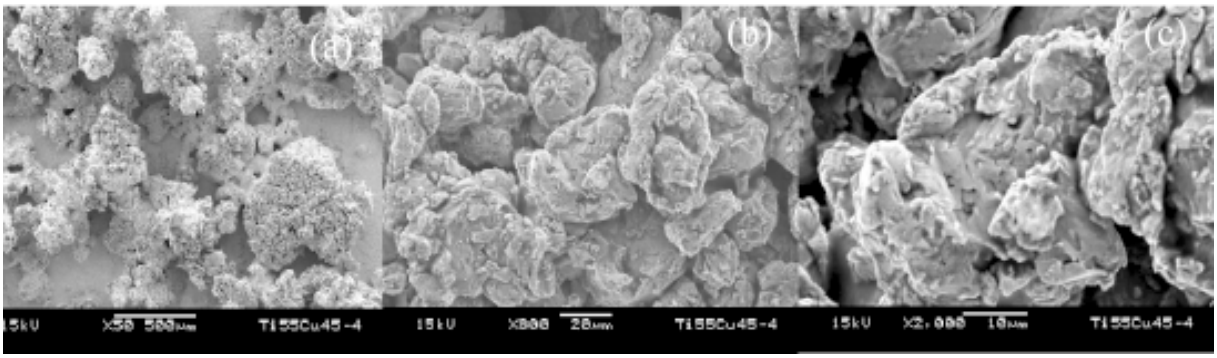

Fig. 5. SEM images of the $Cu_{45}Ti_{55}$ sample after 4 h of MA time at different magnifications.

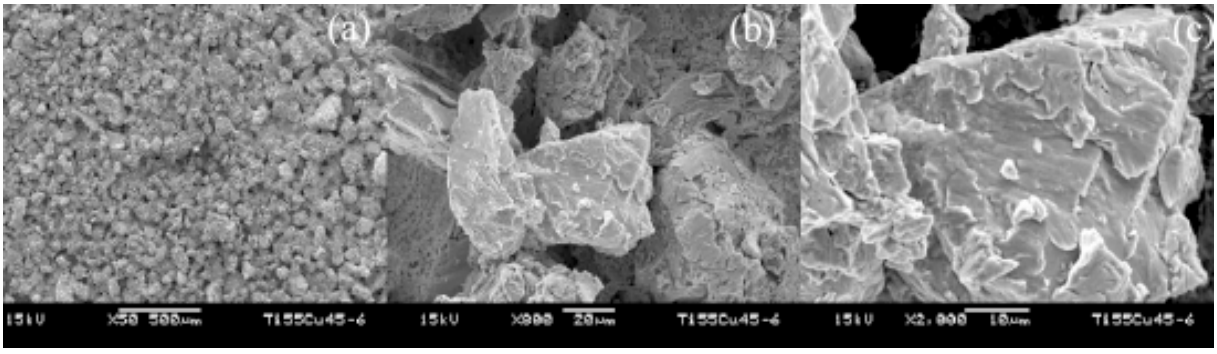

Fig. 6. SEM images of the $Cu_{45}Ti_{55}$ sample after 6 h of MA time at different magnifications.

type particles as well as the flakes that form Ti particles (Figs. 4b and 4c). Chemical analysis (Table 1) shows that alloying occurred as the particles contain both Ti and Cu. However, the amount of both

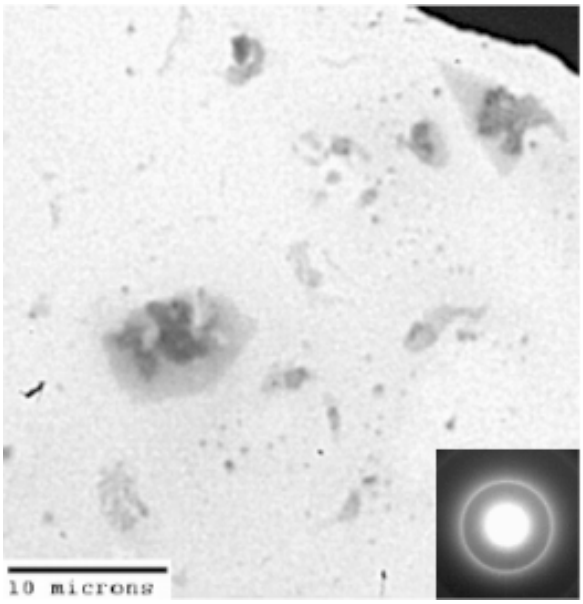

Fig. 7. Typical TEM image and the diffraction pattern of $Cu_{45}Ti_{55}$ sample at 6 h of MA time.

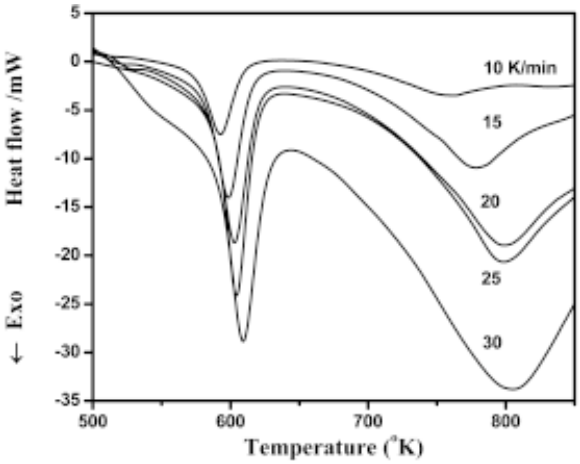

Fig. 8. DSC curves of $Cu_{45}Ti_{55}$ sample at different heating rates**.**

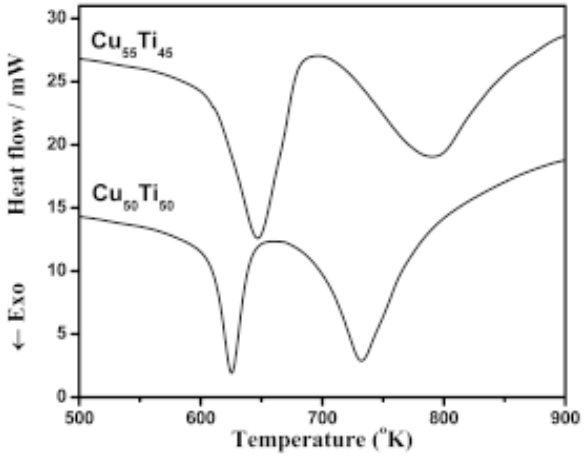

Fig. 9. DSC curves of $Cu_{50}Ti_{50}$ and $Cu_{55}Ti_{45}$ with heating rate of 25 K/min.

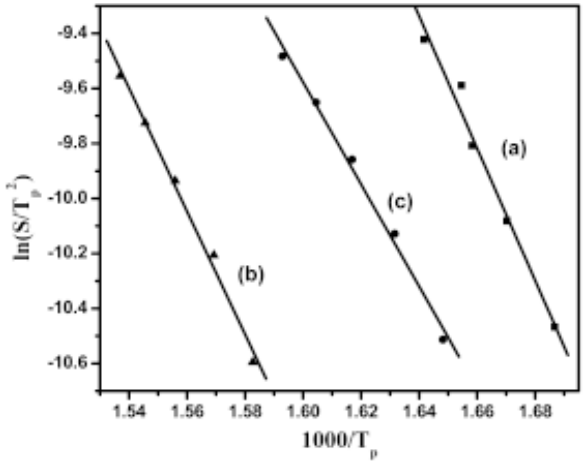

Fig. 10. Plot of the ln(*S*/*Tp*) vs. (1000/*Tp*) of the: (a) $Cu_{45}Ti_{55}$,(b) $Cu_{50}Ti_{50}$, and (c) $Cu_{55}Ti_{45}$ samples.

Cu and Ti vary from one particle to another. By increasing the milling time (at 4 h), the mixture powders show the formation of a sponge-type large particles (Fig. 5). At higher magnification, we can see clearly the formation of agglomerates of fine particles less than 50 μm as shown in Figs. 5b and 5c. Chemical analysis reveals much better homogeneity compared to that obtained after 2 hours of milling (see Table 1). Further MA milling up to 6 hours result in the disappearance of the sponge-type particles with a better particle size distribution (Fig. 6). At higher magnification, a lamellar composite can be observed (Figs. 6b and 6c) which is consistent with the results previously reported for the amorphous materials [19,20]. Chemical analysis shows the amounts of both Cu and Ti (Table 1) which are close to the starting composition. As shown in Fig. 7 the amorphous $Cu_{45}Ti_{55}$ phase was further confirmed by TEM analysis. The typical TEM image shows no crystalline phase, and the diffraction pattern shows a diffuse halo ring, which is a characteristic of amorphous phase.

3.3. Alloy thermal stability

To study the crystallization behavior of the amorphous $Cu_{45+x}Ti_{55-x}$ powders, DSC measurements at different heating rates (10, 15, 20, 25, and 30 K/min) were carried out. It has been found that, all the DSC curves show the presence of two main

exothermic peaks for all the samples, where the peak temperature and the heat flow vary with the different heating rate. Fig. 8 shows the DSC traces of the amorphous $Cu_{45}Ti_{55}$ powder as a function of temperature at different heating rate. The first exothermic peak which is sharp and well-defined vary from 592.84 to 604.36K depending on the increase on the heating rate. Also can be seen, the second exothermic peak which is very broad peak at temperatures which vary from 757 to 805.01K. A similar observation was previously obtained for $Cu_{40}Ti_{60}$ and $Cu_{60}Ti_{40}$ samples prepared by melt spinning technique, in which the crystallization process occurred in two steps for Ti-containing alloys. [11]. The amorphous $Cu_{50}Ti_{50}$ and $Cu_{55}Ti_{45}$ powders, in the present work, revealed the same observations at different heating rates. As an example, Fig. 9 shows the DSC carves for the amorphous $Cu_{50}Ti_{50}$ and $Cu_{55}Ti_{45}$ powders at a heating rate of 25 K/min. The only difference is that, the thermal stability increases with Cu concentration. Table 2 summarizes the values of the first peak of crystallization temperature (T_{p1}) for all these amorphous samples at different heating rates. It is clear that, the value of the peak crystallization temperature increases with the increase of the heating rate and the increase of the copper content. These results were confirmed by diffraction experiments for the Cu-Ti alloys in which the extent of chemical short range order increases with copper content [10]. This leads to a conclusion that the thermal stability of $Cu_{45+x}Ti_{55-x}$ samples, prepared by MA technique, increases with the increase of copper content. On the other hand, these results contradict with that obtained by Rohit Jain *et al*. for $Cu_{50}Ti_{50}$ sample prepared by melt-quenching technique, where they reported that the thermal stability of the $Cu_{50}Ti_{50}$ composition is higher than that of $Cu_{43}Ti_{57}$ and $Cu_{53}Ti_{47}$ compositions [12].

Since, the crystallization temperature depends strongly on the heating rate process [21], more information on the crystallization kinetics of $Cu_{45+x}Ti_{55-x}$ powders may be estimated by the Kissinger equation [22]

$$\ln\left(S / T_p^2\right) = -E_a / RT_p + \text{constant},$$

where S is the heating rate; E_a the activation energy; R the gas constant and T_p is the peak temperature. A plot of $\text{Ln}(S/T^2_p)$ against $10^3/T_p$ gives the activation energy of crystallization E_a. Fig. 10 shows $\text{Ln}(S/T^2_p)$ against $10^3/T_p$ of the amorphous $Cu_{45}Ti_{55,}$ $Cu_{50}Ti_{50}$ and $Cu_{55}Ti_{45}$ powders. From the slope of the straight lines of this figure, the values of E_a of the three samples can be deduced. Table 3 summarizes E_a values for such samples.

It should be pointed out that the E_a values obtained for the present amorphous $Cu_{45}Ti_{55}$, $Cu_{50}Ti_{50}$ and $Cu_{55}Ti_{45}$ powders are much lower (about 1/3) than that obtained for some other metallic glasses and metal-metalloid glasses [23]. It may be a coincidence but should be noted that all the $Cu_{45}Ti_{55}$, $Cu_{50}Ti_{50}$ and $Cu_{55}Ti_{45}$ samples transferred to a complete amorphous phase at low milling time than that reported for other system. Hence, the crystallization activation energy for the present samples seems to be much lower than that observed for other systems.

4. CONCLUSION

In this study, $Cu_{45}Ti_{55}$, $Cu_{50}Ti_{50}$, and $Cu_{55}Ti_{45}$ samples were prepared by MA technique at different periods of time. XRD diffraction patterns show clearly the evolution of the structure of the starting pure elements Cu and Ti with the milling time. The intensity of the diffraction, in particular of Cu, decreases drastically after 2 hours of MA time. All the Bragg peaks of these samples vanished after 6 hours of milling time. The position of the amorphous halo depends on the amount of the copper concentration on the specimens. This evolution of the structure of such samples has been confirmed by SEM analysis at different milling time; reduction of the particle size, formation of agglomerates and then lamellar structure which could be an evidence of the presence of amorphous phase. TEM analysis emphasized that the final structure of these samples after 6h of MA time is genuine. DSC measurements showed that the thermal stability of the amorphous $Cu_{45+x}Ti_{55-x}$ powders increases as the copper content increases. The low activation energies obtained for these samples reflect the fast transformation from crystal to amorphous phase.

REFERENCES

[1] X. L Yeh, K. Samwer and W. L Johnson // *J. Appl. Phys*. **60** (1987) 124.
[2] X. L Yeh, K. Samwer and W. L Johnson // *Appl. Phys. Lett.* **42** (1983) 3.
[3] M. S. Al-Assiri, A. Al-Hajry and N. Cowlam // *J. Physica B* **270** (1999) 125.
[4] A. Ye. Yermakov, V. A. Barinov and Ye. Ye. Yurchikov // *Fiz. Met. Metallov.* **54** (1982) 935.
[5] A. Al-Hajry, M. S. Al-Assiri and N. Cowlam // *J. Phys. Chem. Solids.* **59** (1998) 1499.

[6] Li Meiya, S. Enzo, I. Soletta, N. Cowlam and G. Cocco // *J. Phys. Cond. Matter* **5** (1993) 5235.
[7] A. A. Soliman, S. Al-Hemiti, A. Al-Hajry, M. Al-Assiri and G. Baracati // *Thermochimica Acta* **413** (2004) 57.
[8] Y. J. :Yang, D. W. Xing, J. Shen, J. F. Sun, S. D. Wei, H. J. He and D. G.McCarney // *J. of Alloys and Compounds* **415** (2006) 106.
[9] S. Suzuki, K. Hirabayashi, H. Shibata, K. Mimura, M. Isshiki and Y. Waseda // *Scripta Materialia* **48** (2003) 431.
[10] N. Sakata, N. Cowlam, H. A. Davies, In: *Proceedings of the Fourth International Conference on Rapidly Quenched Metals* ed. by A. Masumotto and K. Suzuki (1982), p. 327.
[11] K. Brunelli, M. Dabala, R. Frattini, G. Sandona and I. Calliari // *J. of Alloys and Compounds* **317-318** (2001) 595.
[12] Rohit Jain, N. S. Saxena, Deepika Bhandari, S. K. Sharma and K. V. R. Rao // *Physica B* **301** (2001) 341.
[13] F. Delogu and G. Cocco // *J of Alloys and Compounds* **352** (2003) 92.
[14] L. Schultz, E. Hellstern and A. Thoma // *Europhys. Lett* **3** (1987) 921.
[15] P. Petzoldt, B. Scholz and H. D. Kunze // *Mater. Sci. Eng.* **97** (1988) 25.
[16] M. Al-Assiri, A. Al-Hajry, J. Hefne, A. Al-Shahrani, S. Abboudy, S. Al-Heniti and N. Cowlam // *Journal of metastable and Nanocrystalline* **8** (2000) 732.
[17] A. Al-Hajry, M. Al-Assiri, S. Enzo, N. Cowlam, J. Hefne , L. Jones, F. Delogu and H. Brequel // *Journal of metastable and Nanocrystalline* **13** (2002) 211.
[18] M. S. Al-Assiri // *J. Phys. Chem. Solids*, in press.
[19] S. Venkataraman, E. Rozhkova, J. Eckert, L. Schultz and D. J. Sordelet // *Intermetallics* **13** (2005) 833.
[20] Pee-Yew Lee, Ju-Lung, Chung-Kwei Lin and Hong-Ming Lin // *Metalu. and Materia. Transactions A* **28A** (1997) 1429.
[21] A. Pratap, A. Prasad, S. R. Joshi, N. S. Saxena, M. P. Saksena and K. Amiya // *Mat. Sci. Forum* **179-181** (1995) 851.
[22] H. E. Kissinger // *Anal. Chem.* **29** (1957) 1702.
[23] G. K. Dey, E. G. Baburaj and S. Banerjee // *J. Mat. Sci.* **21** (1986) 117.